JOURNAL OF MATERIALS SCIENCE 25 (1990) 3910–3916

Electrical resistivity changes due to interstitial hydrogen in palladium-rich substitutional alloys

K. BABA, U. MIYAGAWA, K. WATANABE, Y. SAKAMOTO
Department of Materials Science and Engineering, Nagasaki University, Nagasaki 852, Japan
T. B. FLANAGAN
Department of Chemistry, The University of Vermont, Burlington, Vermont 05405, USA

The changes in electrical resistivity of palladium solid solution alloys (alloying element = silver, gold, copper, yttrium, cerium, titanium, zirconium, vanadium, niobium and tantalum) with hydrogen concentration were measured at 301 K up to about $r(H/M) = 1.5 \times 10^{-2}$; the hydrogen was introduced by electrolysis and measurements of electrode potential were also made. The specific electrical resistivity increment per unit change of hydrogen concentration, $\partial\Delta\rho/\partial r$, generally increases with increase of the solute contents, although for silver, gold and copper there are no notable changes in the slopes with their concentrations. The increase in $\partial\Delta\rho/\partial r$ with the alloying contents cannot be related to the lattice "dilatation" effect due to the solute, but it is associated approximately with a decrease in the density-of-states at the Fermi level caused by pre-filling of the 4 d band of palladium by the solute atoms.

1. Introduction

A number of studies on the effect of dissolved hydrogen on the electrical resistivity of palladium and palladium alloys has been carried out at or near room temperature in conjunction with measurements of p–c–T relationships, where p is the pressure, c the concentration and T the temperature, in order to examine the solubility behaviour of hydrogen over a wide range of hydrogen concentrations, including α, $\alpha + \beta$ (α') and β (α') phases [1–3]. The relationships between relative electrical resistance, R/R_0, and hydrogen content, r(H/M), where R is the electrical resistance at a given hydrogen content and R_0 is the hydrogen-free resistance are found to exhibit different behaviour for various palladium alloys.

With increase of substitutional content in the region of relatively low contents, the Pd–Pt [4, 5], Pd–Ni [6], Pd–Ir [7], Pd–V [8], Pd–Nb [9] and Pd–Ce [9] alloys exhibit initially a gradually steeper increase of R/R_0 than pure palladium with increasing hydrogen content over the region of α and ($\alpha + \beta$) phases, although when the ratios are again compared within the more limited range of very low hydrogen concentrations of the α-phase, the alloys such as the Pd–V [8] and Pd–Ce [10] exhibit rather a less steep increase of R/R_0 against r with increasing solute contents. Furthermore, for several of these alloys, there is a definite change of slope, $\partial(R/R_0)/\partial r$, at the limiting concentration of α-phase (α_{max}), and then R/R_0 passes through a maximum corresponding to the completion of the β-phase transition (β_{min}) like pure palladium [1–3]. When substituted into palladium, some of these solute metals contract the host lattice (nickel, iridium, vanadium) and some expand the host lattice (platinum, niobium and cerium).

In the cases of Pd–Ag [11], Pd–Au [12], Pd–Rh [6], Pd–Pb [13] and Pd–Cu [14] alloys, values of R/R_0 increase less steeply as a function of hydrogen content with increase of substituted metal content. Silver, gold and lead expand the host palladium lattice, and copper and rhodium contract it. It has been reported [15], however, that these resistivity relationships for the Pd–Cu alloys were virtually the same as for pure palladium, i.e. within experimental error there was no trend in the relationships with the copper contents. For the Pd–Ag alloys [11] containing about 20 to 30 at % Ag, the R/R_0 relationships exhibit maxima and minima as a function of hydrogen content, and R/R_0 values for alloys containing about 40 to 50 at % Ag decrease with hydrogen content.

Thus the electrical resistance changes as a function of hydrogen content in the palladium-rich alloys which have been examined do not appear to be simply correlated with the "expanded"–"contracted" lattice classification of palladium alloys [7–9, 13–21] noted earlier with regard to their ability to absorb hydrogen. The resistance–hydrogen content behaviour for the palladium alloys should reflect information about the electronic structure, in addition to the lattice distortion effect, because there should be an effect due to the electron donation by the hydrogen atom on the d band of the alloys. The relationships of electrical resistance, R, with r as $r \to 0$ are free from complications introduced by the $(1 - r)$ factor which appears in Nordheim's rule [22], i.e. $R \propto r(1 - r)$, where r is the atom fraction of interstitial hydrogen computed on the basis of unoccupied and occupied interstices. At low hydrogen contents, the complications introduced by the formation of a second non-stoichiometric hydride phase are absent.

0022–2461/90 $03.00 + .12

Flanagan *et al.* [14] and Smith and Harris [10] have pointed out that rather than examining changes of R/R_0 with r, the absolute changes of resistivity, $\Delta\rho = \rho - \rho_0$, should be determined, where ρ is the specific electrical resistivity at a particular $r = H/M$ and ρ_0 is the specific resistivity in the hydrogen-free state, because the presentation of R/R_0 against r introduces changes due to variation of R_0 from alloy-to-alloy although values of $\partial\Delta\rho/\partial r$ themselves may be relatively constant. Presentation of data as R/R_0–r therefore masks some details about the fundamental nature of the resistivity changes when intercomparing alloys and may make comparisons misleading.

The aim of this study is to obtain more detailed information about the variation of the specific electrical resistance as a function of hydrogen concentration in the lower hydrogen content of α-phase of palladium solid solution alloys some of whose resistivity relationships have not been previously examined, i.e. Pd–Ti and Pd–Zr.

2. Experimental procedure

The palladium solid solution alloys used were prepared by arc melting under an argon atmosphere. The purity of the starting metals was as follows (wt %); Pd 99.98, Ag 99.99, Au 99.99, Cu 99.99, Y 99.9, Ce 99.9, Ti > 99.5, Zr > 99.6, V > 99.7, Nb > 99.5 and Ta 99.9. The alloy buttons were annealed for homogenization and then rolled to foils of thickness 100 to 120 μm. Samples for electrical resistance measurements were cut from the foils so that their dimensions were about 2 mm × 30 mm. Finally, all the samples were annealed at 1123 K for 2 h *in vacuo*, and then furnace-cooled to room temperature at a rate of 5 to 6 K min^{-1}.

Under the final annealing treatment, as the Pd–12.5 at % Ce alloy forms a long-range Pt_7Cu-type ordered structure [23–25], and the alloys of the Pd–8.0 and 10.0 at % Y also form the same type of short-range ordered structure [26], some of these alloy samples were quenched by the following treatment: the samples were wrapped in zirconium foil, sealed-off in evacuated silica tubes, heated to about 1192 K for 7 min and then quenched into ice–water while simultaneously breaking the container. The quenched Pd–12.5 at % Ce alloy was still in the short-range ordered state.

The changes of electrode potential and electrical resistance resulting from an electrolytic introduction of known hydrogen concentrations were measured with the apparatus described previously [27]. As an electrolyte, a highly viscous liquid containing two parts by volume of glycerine with one part by volume of phosphoric acid (85 wt %) was used to charge the samples with hydrogen. All the measurements were carried out at 301 K. Before carrying out the e.m.f. and electrical resistance measurements, the sample surfaces were etched with a solution of H_2SO_4 : HNO_3 : H_2O = 2 : 2 : 1 mixture. Thin nickel lead wires were spot-welded to samples for the electrical resistivity measurement by the four-points technique. After immersing the sample electrode in the electrolyte, hydrogen introduced during etching was removed by applying an anodic potential of 500 mV against an Ag/AgCl reference electrode for about 12 h. Hydrogen was introduced into the sample by passing a short current pulse, i_0 = 2 to 20 mA, from the platinum counter-electrode to the sample. The hydrogen concentration, defined as the atomic ratio of hydrogen-to-metal (H/M), was calculated from Faraday's law. Starting with small amounts of hydrogen, the concentration was increased stepwise until bubbles of hydrogen formed at the sample surface. After each step when the electrode potential achieved a constant value, the resistance was measured by a digital voltmeter.

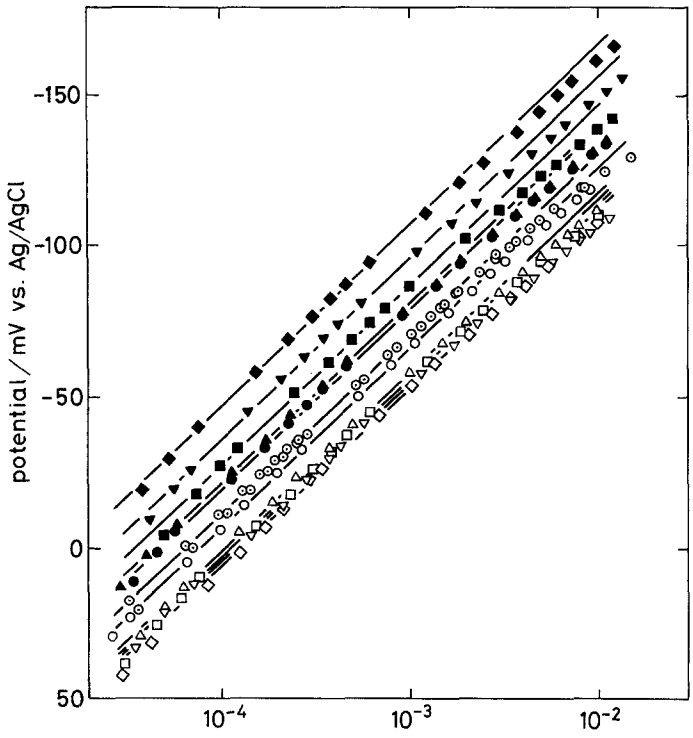

Figure 1 Potentials of hydrogen-introduced Pd–Ti and Pd–Zr alloys plotted against the hydrogen concentration, in comparison with that of (⊙) well-annealed pure palladium at 301 K [27]. Ti (at %): (●) 2, (▲) 4, (■) 6, (▼) 8, (◆) 10. Zr (at %): (○) 2, (△) 4, (□) 6, (▽) 8, (◇) 10.

TABLE I Electrical resistivity, ρ_0, of the hydrogen-free palladium solid solution alloys and the resistivity increment per unit change of hydrogen concentration, $\partial\Delta\rho/\partial r$, and $\partial(R - R_0)/R_0/\partial r$ at 301 K, where $\Delta\rho = \rho - \rho_0$, and the hydrogen concentration range: $\sim r(\mathrm{H/M}) = 1.5 \times 10^{-2}$. a_{ss} = lattice parameter of the hydrogen-free alloys

Alloys	a_{ss} (± 0.0001 nm)	ρ_0 ($10^{-5}\,\Omega$ cm)	$\partial\Delta\rho/\partial r$ ($10^{-5}\,\Omega$ cm)	$\partial(R - R_0)/R_0/\partial r$
Pd	0.3890	1.24	4.6	3.7
Pd–3.0 at % Ag	0.3896	1.63	4.6	2.8
Pd–6.0 at % Ag	0.3902	2.04	4.9	2.4
Pd–9.9 at % Ag	0.3911	2.48	4.0	1.6
Pd–3.0 at % Au	0.3896	1.34	4.1	3.1
Pd–6.0 at % Au	0.3904	1.52	3.9	2.6
Pd–10.0 at % Au	0.3911	2.01	3.9	1.9
Pd–5.0 at % Cu	0.3878	1.90	4.8	2.5
Pd–10.1 at % Cu	0.3866	2.49	4.4	1.8
Pd–13.4 at % Cu	0.3861	3.18	4.8	1.5
Pd–2.0 at % Y	0.3903	1.92	6.3	3.3
Pd–3.9 at % Y	0.3918	2.62	7.5	2.9
Pd–6.0 at % Y	0.3931	3.05	8.2	2.7
Pd–8.0 at % Y	0.3943	3.81	11.2	2.9
Pd–10.0 at % Y	0.3957	4.46	15.9	3.6
Pd–2.0 at % Ce	0.3905	1.77	4.9	2.8
Pd–4.0 at % Ce	0.3921	2.49	5.8	2.3
Pd–6.0 at % Ce	0.3936	3.42	7.4	2.2
Pd–8.0 at % Ce	0.3951	4.41	8.4	1.9
Pd–10.0 at % Ce	0.3968	5.37	12.9	2.4
Pd–12.5 at % Ce (quenched)	0.3991	9.76	39.2	4.0
Pd–12.5 at % Ce (annealed)	0.3985	2.07	15.5	7.5
Pd–2.0 at % Ti	0.3889	1.76	4.8	2.7
Pd–4.0 at % Ti	0.3888	2.32	5.6	2.4
Pd–6.0 at % Ti	0.3888	2.96	6.5	2.2
Pd–8.0 at % Ti	0.3887	3.80	8.5	2.2
Pd–10.0 at % Ti	0.3887	4.62	12.4	2.7
Pd–2.0 at % Zr	0.3897	1.72	5.1	3.0
Pd–4.0 at % Zr	0.3905	2.42	6.0	2.5
Pd–6.0 at % Zr	0.3912	2.77	6.4	2.3
Pd–8.0 at % Zr	0.3920	3.49	8.4	2.4
Pd–10.0 at % Zr	0.3927	4.38	14.3	3.3
Pd–2.5 at % V	0.3885	1.88	5.8	3.1
Pd–5.0 at % V	0.3881	3.22	7.6	2.4
Pd–7.6 at % V	0.3876	5.36	12.9	2.4
Pd–10.0 at % V	0.3874	7.73	19.4	2.5
Pd–2.0 at % Nb	0.3892	1.77	5.0	2.8
Pd–4.0 at % Nb	0.3894	2.43	5.7	2.3
Pd–6.0 at % Nb	0.3896	3.37	6.5	1.9
Pd–8.0 at % Nb	0.3897	4.27	9.4	2.2
Pd–2.0 at % Ta	0.3892	1.68	4.5	2.7
Pd–4.0 at % Ta	0.3893	2.31	5.0	2.2
Pd–6.0 at % Ta	0.3894	2.96	5.3	1.8
Pd–8.0 at % Ta	0.3898	3.89	8.1	2.1

3. Results and discussion

Typical results of successive measurements of the electrode potentials at increasing hydrogen concentrations are shown in Fig. 1 for the Pd–Ti and Pd–Zr alloys, in comparison with that of well-annealed pure palladium [27]. For all the alloy compositions, plots of e.m.f. against log r give straight lines with a theoretical slope of $2.303\,RT/F = 59.7$ mV at 301 K, except for the hydrogen concentrations above about $r = 2.5 \times 10^{-3}$, and also for very dilute hydrogen contents. Thus, it can be seen that at a constant e.m.f. which corresponds to a constant equilibrium hydrogen pressure, the hydrogen solubility in the Pd–Ti alloys decreases with alloying content, whereas the solubility in the Pd–Zr alloys increases with the alloying content. With the exceptions of the Pd–12.5 at % Ce alloys in the composition range up to 12.5 at % Ce, and of the Pd–Nb(Ta) alloys with more than 4 at % Nb(Ta), the lattice "expanded"–"contracted" classification of palladium alloys, based on their ability to absorb hydrogen, was obeyed for the other alloys studied in this work; the "expanded" alloys studied are Pd–Ag, Pd–Au, Pd–Y, Pd–Ce, Pd–Nb and Pd–Ta, and the "contracted" alloys are Pd–Cu and Pd–V. Hydrogen solubility in the Pd–Nb(Ta) alloys exhibited a minor maximum at 2.0 at % Nb(Ta), and then decreased with the solute metal content. The solubility behaviour is quite analogous to the trends noted earlier for

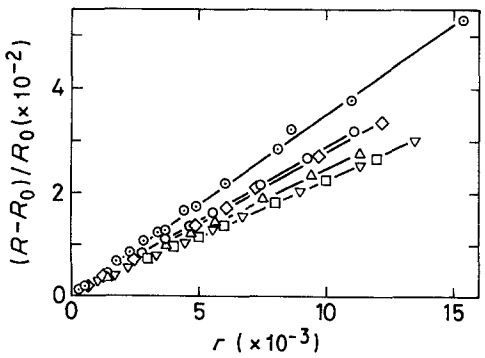

Figure 2 Relationships of $(R-R_0)/R_0$ plotted against r during absorption of hydrogen for the Pd–Ti alloys at 301 K. (⊙) Well-annealed palladium [27]. Ti (at %): (○) 2, (△) 4, (□) 6, (▽) 8, (◇) 10.

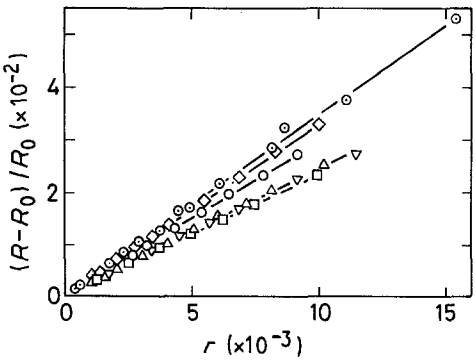

Figure 3 Relationships of $(R-R_0)/R_0$ plotted against r during absorption of hydrogen for the Pd–Zr alloys at 301 K. (⊙) Well-annealed palladium [27]. Zr (at %): (○) 2, (△) 4, (□) 6, (▽) 8, (◇) 10.

"expanded"–"contracted" palladium alloys determined from p–c–T measurements using gaseous hydrogen [7–8, 13–21, 28]. The quenched Pd–12.5 at % Ce alloy dissolved more hydrogen than the ordered form as shown previously [25].

The specific electrical resistivity, ρ_0, of the hydrogen-free alloys determined at 301 K are given in Table I. The ρ_0 values of each alloy increase more or less with increasing alloying contents; they are in good agreement with the published data [14, 29–31]. Data of the Pd–Ce, Pd–Y and Pd–Ti alloys were not found in the literature. The resistivity value of the quenched (short-range ordered) Pd–12.5 at % Ce alloy was about five times greater than that of the annealed (ordered) alloy, which agrees with the previously reported value [25].

It was found that the electrical resistance, R, of all of the alloys increases almost linearly with hydrogen content up to about $r = 1.5 \times 10^{-2}$, except for the ordered Pd–12.5 at % Ce alloy. This ordered alloy exhibited a gradually increasing slope of R with increasing hydrogen content. It is not known why the ordered alloy behaves in this manner nor is it known whether other ordered alloys behave similarly [27]. These resistance data were converted to the specific resistivity.

Representative data plots of $(R - R_0)/R_0$ against r for the Pd–Ti, Pd–Zr and Pd–Ce alloys are shown in Figs 2 to 4, respectively. It can be seen that the slopes, $\partial(R - R_0)/R_0/\partial r$, initially decrease with the solute contents up to about 6 to 8 at %, and then increase with metal solute content. Similar results were observed for the other palladium alloys, except for the Pd–Ag, Pd–Au and Pd–Cu alloys in which the slopes exhibited only a gradual decrease with the metal solute contents. The trends of the initial decrease in the $\partial(R - R_0)/R_0/\partial r$ value with alloying metal content at relatively low solute content alloys are in agreement with those of the previously measured alloys, e.g. Pd–Ag [11], Pd–Au [12], Pd–Rh [6], Pd–Pb [13], Pd–Cu [14], Pd–V [8] and Pd–Ce [10], etc.

Figs 5 to 7 show plots of $\Delta\rho$ $(=\rho - \rho_0)$ against r for the Pd–Ti, Pd–Zr and Pd–Ce alloys. There is also an approximately linear variation of $\Delta\rho$ with r, which passes through the origin, and the slopes of $\partial\Delta\rho/\partial r$

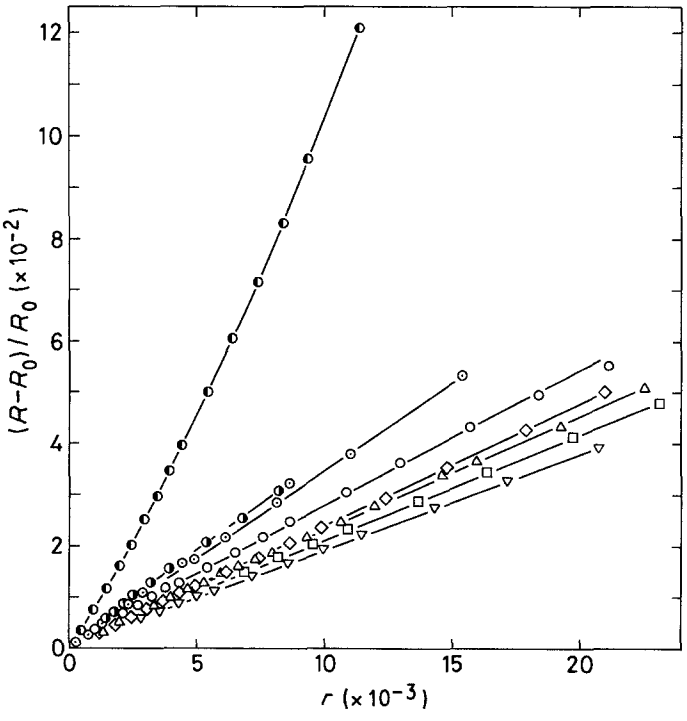

Figure 4 Relationships of $(R-R_0)/R_0$ plotted against r during absorption of hydrogen for the Pd–Ce alloys at 301 K. (⊙) Well-annealed palladium [27]. Ce (at %): (○) 2, (△) 4, (□) 6, (▽) 8, (◇) 10, (◑) 12.5 quenched, (◐) 12.5 annealed.

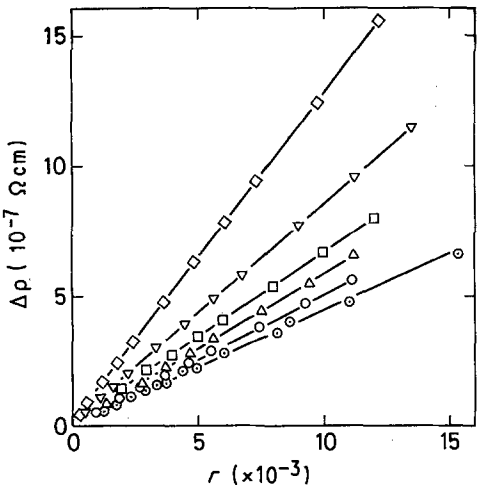

Figure 5 Relationships of $\Delta\rho$ plotted against r during absorption of hydrogen for the Pd–Ti alloys at 301 K. (⊙) Well-annealed palladium [27]. Ti (at %): (○) 2, (△) 4, (□) 6, (▽) 8, (◇) 10.

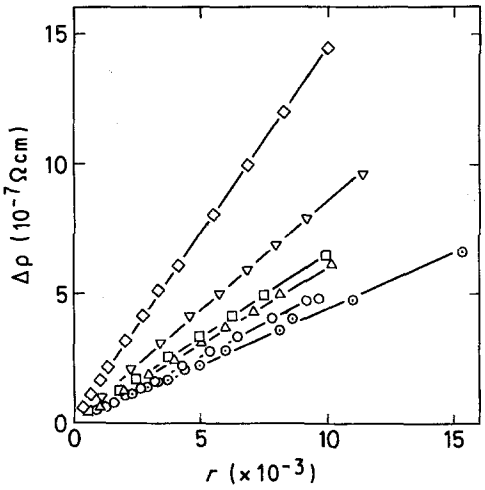

Figure 6 Relationships of $\Delta\rho$ plotted against r during absorption of hydrogen for the Pd–Zr alloys at 301 K. (⊙) Well-annealed palladium [27]. Zr (at %): (○) 2, (△) 4, (□) 6, (▽) 8, (◇) 10.

increase with an increase of the metal solute contents in the alloys. Similar results were also observed for the other Pd alloys, although for the alloys of Pd–Ag, Pd–Au and Pd–Cu, there was no remarkable change in the slopes, rather the slopes decreased slightly for the Pd–Au alloys, and/or they remained almost constant for the Pd–Ag and Pd–Cu alloys.

The specific electrical resistivity increment per unit change of hydrogen concentration $\partial\Delta\rho/\partial r$ for all the alloys are summarized in Table I, together with the $\partial(R - R_0)/R_0/\partial r$ values, in comparison with those of well-annealed pure palladium [27]. The same table shows the lattice parameter, a_{ss}, of the hydrogen-free alloys. For the ordered Pd–12.5 at % Ce alloy, the slope was estimated from the initial linear portion, i.e. at small hydrogen contents below about $r = 2.5 \times 10^{-3}$. As mentioned above presenting data only via the conventional plots of $(R - R_0)/R_0$ with r would mask some fundamental aspects of the resistivity changes due to dissolved hydrogen when comparing alloys.

In order to correlate variations in $\partial\Delta\rho/\partial r$ with the properties of the different alloys, the slopes were plotted against the unit cell volume change, ΔV, of the alloys as shown in Fig. 8, where $\Delta V = V_s - V_{Pd}$ and V_s is the unit cell volume of the hydrogen-free solid solution alloys and V_{Pd} is that of pure palladium. The unit cell volumes were calculated from the lattice parameters [32–34]. As can be seen from Fig. 8 there seems to be no correlation of the values of $\partial\Delta\rho/\partial r$ with

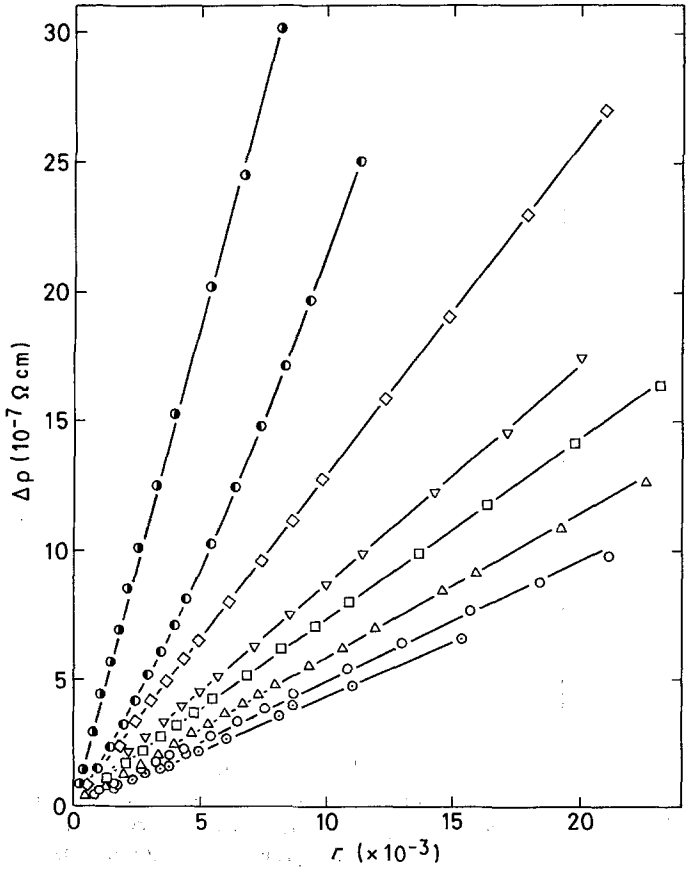

Figure 7 Relationships of $\Delta\rho$ plotted against r during absorption of hydrogen for the Pd–Ce alloys at 301 K. (⊙) Well-annealed palladium [27]. Ce (at %): (○) 2, (△) 4, (□) 6, (▽) 8, (◇) 10, (◑) 12.5 quenched, (◐) 12.5 annealed.

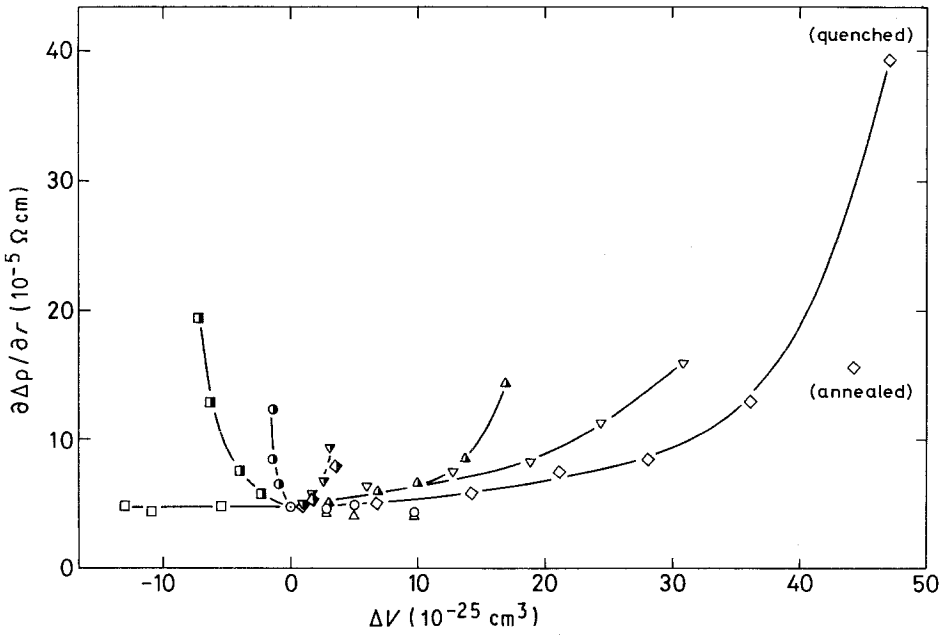

Figure 8 Variation of $\partial\Delta\rho/\partial r$ with change in unit cell volume, ΔV, of the palladium alloys due to the solute atoms. (⊙) Pd, (○) Ag, (△) Au, (□) Cu, (▽) Y, (◇) Ce, (◑) Ti, (◭) Zr, (◨) V, (▼) Nb, (◆) Ta.

whether the alloy is an "expanded" ($\Delta V > 0$) or "contracted" ($\Delta V < 0$) alloy, although the slopes of the Pd–Ag and Pd–Cu alloys remain almost constant, and for the Pd–Au alloys the slopes decrease slightly with the alloying contents.

It may be seen from Fig. 8 that there is roughly a trend towards a steeply increasing effect of hydrogen on the $\Delta\rho$ value as the valence electron concentration, e/a, of the hydrogen-free alloys increases at the same ΔV values. This suggests that the solute atoms of silver, gold and copper have similar effects on the variations of $\partial\Delta\rho/\partial r$, whereas the other solute atoms have larger effects compared to these three alloys. It is possible that this is related to the donation of one electron by silver, gold and copper to the 4 d band of palladium and on this basis the other solute atoms donate more electrons, although the rigid band model is no longer believed to be fully valid.

Fig. 9 shows the relationship between the $\partial\Delta\rho/\partial r$ and valence electron concentration, e/a, for the initial hydrogen-free alloys. Here the assumed valencies are 3 for yttrium, 4 for titanium, zirconium and cerium and 5 for vanadium, niobium and tantalum [30]. There is an approximately linear increase of $\partial\Delta\rho/\partial r$ with valence electron concentration, although the $\partial\Delta\rho/\partial r$ values of the Pd–Y alloys are somewhat high. Thus the rise in the electrical resistivity, $\Delta\rho$, of the alloys with hydrogen addition is related at least phenomenologically to a decrease in the density-of-states at the Fermi level by progressively pre-filling of the 4 d band of palladium with the electron from the solute atoms. The difference in the $\partial\Delta\rho/\partial r$ between the annealed (ordered) and quenched (short-range ordered) states of Pd–12.5 at % Ce alloys may be attributed to the changes in the density-of-states at the Fermi level associated with the long-range and short-range ordered conditions.

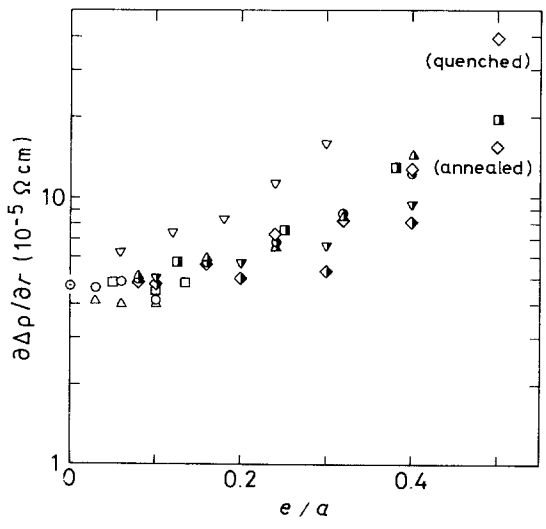

Figure 9 Variation of $\partial\Delta\rho/\partial r$ with valence electron concentration, e/a, for the palladium alloys. For key, see Fig. 8.

4. Conclusions

1. The specific electrical resistivity of hydrogen-free palladium alloys increases more or less with increasing solute contents. The resistivity value of the quenched (short-range ordered) Pd–12.5 at % Ce alloy is about five times greater than that of the ordered state.

2. The electrical resistance, R, of all of the hydrogenated alloys increases almost linearly with hydrogen contents up to about $r = 1.5 \times 10^{-2}$, except for the ordered Pd–12.5 at % Ce alloy. The ordered alloy exhibits a gradually increasing slope of R with increasing hydrogen content.

3. For the conventional plots of $(R - R_0)/R_0$ against r, the slopes, $\partial(R - R_0)/R_0/\partial r$, decrease with the metal solute contents up to about 6 to 8 at % and then increase with further increase of the metal solute content, except for the Pd–Ag, Pd–Au and Pd–Cu alloys, where the slopes show only a gradual decrease with the alloying content. While generally the slopes of $\partial\Delta\rho/\partial r$ in the plots of $\Delta\rho$ against r increase with an increase of the metal solute contents, for the Pd–Ag, Pd–Au and Pd–Cu alloys there is no remarkable change in the slopes. Thus the conventional presentation of $(R - R_0)/R_0$ against r would mask some facts about the fundamental nature of the resistivity

changes due to dissolved hydrogen when comparing alloys.

4. The variation in $\partial\Delta\rho/\partial r$ values with the metal solute contents cannot necessarily be related to the lattice "dilatation" effect but it seems to be associated with a decrease in the density-of-states at the Fermi level, i.e. pre-filling the 4 d band of palladium with the electrons of the solute atoms causes the decrease according to the e/a ratio. The $\partial\Delta\rho/\partial r$ value for the quenched (short-range ordered) Pd–12.5 at % Ce is larger than that of the ordered state.

References

1. F. A. LEWIS, "The Palladium-Hydrogen Systems" (Academic Press, New York, 1967).
2. T. B. FLANAGAN and F. A. LEWIS, *Trans. Faraday Soc.* **55** (1959) 1400.
3. J. C. BARTON, F. A. LEWIS and I. WOODWARD, *ibid.* **59** (1963) 1201.
4. A. W. CARSON, T. B. FLANAGAN and F. A. LEWIS, *ibid.* **56** (1960) 363.
5. B. BARANOWSKI, F. A. LEWIS, W. D. McFALL, S. FILIPEK and T. C. WITHERSPOON, *Proc. Roy. Soc. London* **A386** (1983) 309.
6. J. C. BARTON, J. A. S. GREEN and F. A. LEWIS, *Trans. Faraday Soc.* **62** (1966) 960.
7. M. LaPRADE, K. D. ALLARD, J. F. LYNCH and T. B. FLANAGAN, *J. Chem. Soc. Faraday Trans. I* **70** (1974) 1615.
8. D. ARTMAN, J. F. LYNCH and T. B. FLANAGAN, *J. Less-Common Metals* **45** (1976) 215.
9. K. KANDASAMY, F. A. LEWIS, W. D. McFALL and R. A. McNICHOLL, *Z. Phys. Chem. N.F.*, **163** (1989) 41.
10. D. A. SMITH and I. R. HARRIS, *ibid.* **147** (1986) 1.
11. A. W. CARSON, F. A. LEWIS and W. H. SCHURTER, *Trans. Faraday Soc.* **63** (1967) 1447.
12. A. MAELAND, PhD thesis, University of Vermont (1964).
13. K. D. ALLARD, J. F. LYNCH and T. B. FLANAGAN, *Z. Phys. Chem. N.F.* **93** (1974) 15.
14. D. FISHER, D. M. CHISDES and T. B. FLANAGAN, *J. Solid State Chem.* **20** (1977) 149.
15. R. BURCH and R. G. BUSS, *J. Chem. Soc. Faraday Trans. I* **71** (1975) 913.
16. H. BRODOWSKY and E. POESCHEL, *Z. Phys. Chem. N.F.* **44** (1965) 143.
17. R. BURCH and R. G. BUSS, *J. Chem. Soc. Faraday Trans. I* **71** (1975) 922.
18. R. BURCH and N. B. MASON, *ibid.* **76** (1980) 2285.
19. J. D. CLEWLEY, J. F. LYNCH and T. B. FLANAGAN, *ibid.* **73** (1977) 494.
20. Y. SAKAMOTO, K. KAJIHARA, Y. FUKUSAKI and T. B. FLANAGAN, *Z. Phys. Chem. N.F.* **159** (1988) 61.
21. Y. SAKAMOTO, T. MATSUO, H. SAKAI and T. B. FLANAGAN, *ibid.* **162** (1989) 83.
22. N. F. MOTT and H. JONES, "The Theory of Metals and Alloys" (Oxford University Press, 1935).
23. N. KUWANO, T. SHIWAKU, Y. TOMOKIYO and T. EGUCHI, *Jpn. J. Appl. Phys.* **20** (1981) 1603.
24. D. A. SMITH, I. P. JONES and I. R. HARRIS, *J. Mater. Sci. Lett.* **1** (1982) 463.
25. Y. SAKAMOTO, T. B. FLANAGAN and T. KUJI, *Z. Phys. Chem. N.F.* **143** (1985) 61.
26. Y. SAKAMOTO, M. YOSHIDA and T. B. FLANAGAN, *J. Mater. Res.* **1** (1986) 781.
27. K. BABA, Y. SAKAMOTO and T. B. FLANAGAN, *J. Chem. Soc. Faraday Trans. I* **84** (1988) 459.
28. Y. SAKAMOTO, K. KAJIHARA, T. KIKUMURA and T. B. FLANAGAN, *J. Chem. Soc. Faraday Trans.* **86** (1990) 377.
29. B. SVENSSON, *Ann. Phys.* **14** (1932) 699.
30. E. KUDIELKA-ARTNER and B. B. ARGENT, *Proc. Phys. Soc.* **80** (1962) 1143.
31. Japan Institute of Metals (eds), "Metals Data Hand Book", (Maruzen, Tokyo, 1974).
32. Y. SAKAMOTO, K. YUWASA and K. HIRAYAMA, *J. Less-Common Metals* **88** (1982) 115.
33. Y. SAKAMOTO, H. KANEKO, T. TSUKAHARA and S. HIRATA, *Scripta Metall.* **21** (1987) 415.
34. Y. SAKAMOTO, K. BABA and T. B. FLANAGAN, *Z. Phys. Chem. N.F.* **158** (1988) 223.

Received 18 April
and accepted 13 September 1989